Solubility, Nucleation parameters, Growth and Studies of L-alaninium maleate (LAM) crystals

M.Krishnasamy[1] , S.Subramanian[2], P.Selvarajan[3], D.Shanthi[3]

[1]M.S.University, Tirunelveli, Tamilnadu, India.

[2]Department of Physics, MDT Hindu College, Tirunelveli-10, Tamilnadu.

[3]Department of Physics, Aditanar College of Arts And Science, Tiruchendur-628216, Tamilnadu, India.

Abstract

Organic nonlinear optical (NLO) crystals usually have large NLO efficiency and they are important in providing the key functions of frequency shifting, optical communication, optical storage technology and many other applications. The search for NLO materials reveals that L-alanine based crystals are potential materials for many industrial applications. L-alaninium maleate (LAM) salt was synthesized and solubility studies have been carried out. Nucleation kinetic studies were performed and the single crystals LAM salt were successfully grown by slow evaporation technique. The grown crystals were subjected to various studies like XRD, microhardness studies, measurement of density, measurement of SHG and dielectric studies.

1.Introduction

Most of the amino acids and their complexes are NLO materials that find applications in field of optical communication, photonics, optical data storage etc. Among the amino acids, L-alanine is an acentric crystal and it is a naturally occurring chiral amino acid with a non-reactive hydrophobic methyl group (CH_3) as a side chain. L-alanine molecule exists as a zwitterion, where the carboxyl group is dissociated and amino group is protonated and if it is mixed with different organic acids and inorganic acids to form novel materials, it is

expected to get improved NLO properties[1-3]. Some complexes of L-alanine have been recently crystallized and various studies have been investigated by many researchers[4-7]. In this work, L-alanine is mixed with maleic acid to form L-alanine maleate (LAM) crystal and it is an organic NLO material. Organic NLO materials offer several advantages over inorganic NLO materials such as large nonlinear figure of merit, fast response time and their structural flexibility facilitates easy control of physical properties over very wide range. The crystal structure of L-alaninium maleate (LAM) crystal was solved by Alagar et al [8] and some characterization studies of LAM were found to be reported in the literature[9,10]. The nucleation kinetic studies of LAM sample is reported for the first time and based on the solubility and nucleation kinetic data, the single crystals of LAM were grown. The aim of this paper is to report the systematic studies like solubility, nucleation kinetic studies, growth, XRD studies, microhardness, measurement of density and SHG, dielectric studies of LAM crystals and the results are discussed.

2. Synthesis and solubility

L-alaninium maleate (LAM) salt was synthesized by taking precursor chemicals like AR grade L-alanine and AR grade maleic acid in the molar ratio of 1:1. Calculated amount of the precursor chemicals were dissolved in double distilled water and stirred well using a magnetic stirrer for about 3 hours. The solution was heated until the synthesized salt of LAM was obtained. The purity of the synthesized salt was improved by successive re-crystallization process. The solubility studies were carried out by gravimetrical method [11]. A glass beaker with 25 ml of double distilled water was placed inside a constant temperature bath (accuracy: ±0.01 °C), maintained at 30 ^{o}C. LAM salt was added in small amounts at successive stages. The addition of the salt and the stirring were continued till a small precipitate was formed, which confirmed the supersaturated condition. The 5 ml of the saturated solution was pipetted out and poured into a petri dish of known weight. The solvent

was completely evaporated by warming the solution at 50 °C. The amount of the salt present in 5 ml of the solution was measured and from this, the amount of the salt present in 100 ml of the solution was found out. The solubility trace for LAM sample at different temperatures is shown in the figure 1. It is notice that the solubility increases with temperature and these data will be useful to prepare the saturated and supersaturated solutions and also will be useful to carry out nucleation kinetic studies.

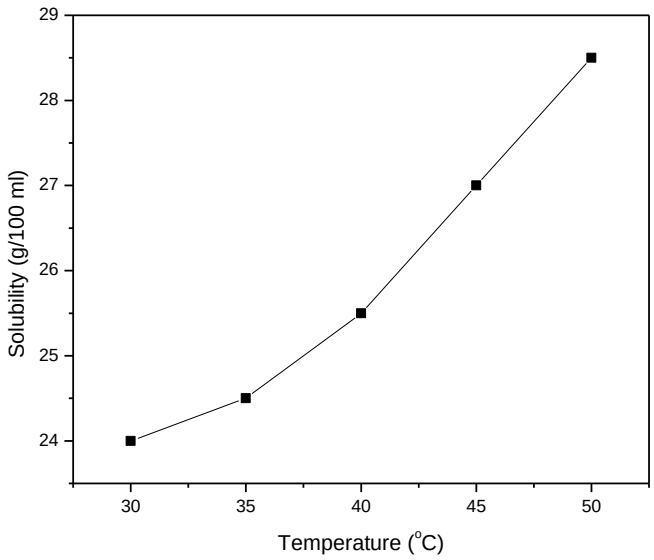

Fig.1: Solubility trace for LAM sample

3. Homogeneous nucleation, induction period and critical parameters

If the nuclei form homogeneously in the interior of the parent phase and in the absence of foreign particles, the occurrence of phase transition is termed as homogeneous nucleation. In homogeneous nucleation, the probability of nucleation occurring at any given site is identical to that at any other site within the assembly. Here the nucleation theory is based on the homogeneous nucleation and when few atoms or molecules are joined together in a supersaturated solution, then a cluster of nucleus is formed and the overall excess Gibbs free energy ΔG between the solute and nucleus is $\Delta G = 4\pi r^2 \sigma + (4/3)\pi r^3 \Delta G_v$ where σ is

the surface energy per unit area, r is the radius of the nucleus and ΔG_v is the free energy per unit volume. This energy is maximum for a certain value of r which is called the critical radius. The volume energy is determined with the help of Thomson-Gibbs equation and is given by $\Delta G_v = -(kT/v) \ln S$. Here the negative sign reveals that transformation of liquid into solid phase, k is the Boltzmann's constant, v is the specific volume of the solute molecule and S is the supersaturation ratio which is calculated from $S = C/C_o$, where C is the supersaturated concentration and C_o is the saturated concentration. Once the nucleation occurs in the supersaturated solution, the nucleus grows quickly and a bright sparkling particle is seen. The time interval between the creation of supersaturation and the formation of critical nuclei is called the induction period(τ). The induction period can be measured for different supersaturation ratio values. A plot of $1/ (\ln S)^2$ against $\ln \tau$ forms a straight line and the slope (m) is calculated. After finding the slope (m), the value of interfacial tension (σ) is calculated from the equation $\sigma = (RT/N) [3m/16\pi v^2]^{1/3}$ where R is the universal gas constant, N is the Avogadro's number and T is the absolute temperature. The net free energy change (ΔG) increases with the increase in size of nucleus, attains maximum and decreases with further increase in the size of nucleus. The size corresponding to the maximum free energy change (ΔG^*) is called critical nucleus. The size of the critical nucleus (r^*) and critical Gibbs free energy change (ΔG^*) are given by $r^* = 2 \sigma v N / RT \, ln \, S$ and $\Delta G^* = mRT / [N (ln \, S)^2]$. Using the value of critical radius, the number of molecules in a critical nucleus is found using the equation $n = (4/3) (\pi/v) r^{*3}$. The number of crystals produced in the supersaturated solution is expressed as nucleation rate i.e. the number of crystals produced per unit volume per unit time and it is calculated using the equation $J = A \exp[-\Delta G^* / (kT)]$ where A is the pre-exponential factor [12].

Experiment for measuring induction period for the sample was performed at selected supersaturation ratios (S), viz. 1.1, 1.13, 1.15 and 1.2 at room temperature (30 ^oC) by

isothermal method [13]. The induction period is influenced by supersaturation, type of solvent, purity of the sample, temperature, pH value of the solution etc. The trace of ln τ with $1/(\ln S)^2$ is shown in the figure 2. The slope (m) is obtained by drawing the best linear fit and from the value of slope (m), the critical nucleation parameters were determined and the values are provided in the table 1.

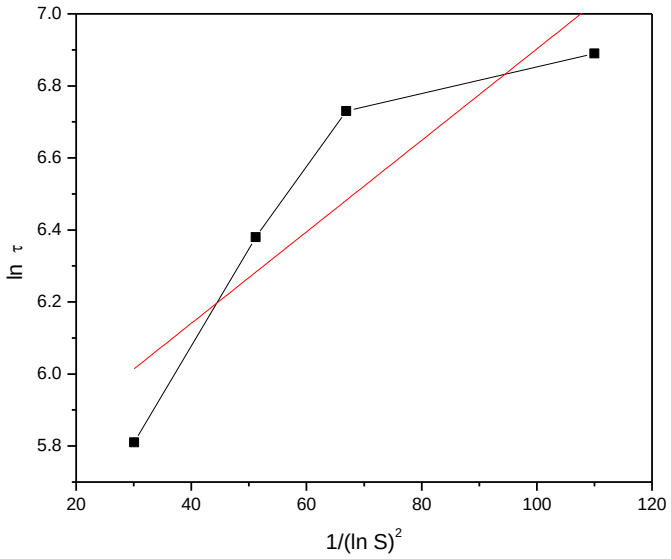

Fig.2: The trace of $1/(\ln S)^2$ versus ln τ LAM salt

Table 1: Critical nucleation values for LAM sample

S	σ x 10^{-3} J/m^2	n	r^* (nm)	ΔG* (kJ/mole)	J x 10^{23} Nuclei/s/vol.
1.1	0.194	31	1.1	3.42	15
1.13		26	0.82	2.73	23
1.15		18	0.74	1.73	32
1.2		10	0.63	1.05	42

From the results it is observed that the induction period decreases with the supersaturation values and the values of ΔG* , n, r* decrease with increase in supersaturation ratio(S). The nucleation rate is found to be increasing with supersaturation ratio and hence formation of multi nuclei in the supersaturated solution could be avoided when low supersaturation ratio is used for the growth of LAM crystals. By controlling nucleation rate, good quality crystals of LAM could be grown and the studies on induction period, interfacial tension, nucleation rate and other nucleation parameters give ideas for the controlled growth of LAM crystals. In this work, the growth of LAM crystals was carried out by taking S=1.1 which gives the low nucleation rate.

4. Growth LAM crystals

L-alaninium maleate (LAM) crystals were grown by solution method with slow evaporation technique. The saturated solution of the re-crystallized salt of LAM was prepared (here S = 1.1) in accordance with the solubility and the optimized nucleation kinetic data. The solution was stirred well using a hot plate magnetic stirrer for 3 hours and it was filtered using a Whatman filter paper. Then the solution was allowed to evaporate and numerous tiny crystals were formed at the bottom of the container due to spontaneous nucleation. It took about 30 days to grow LAM crystals. The harvested crystal of LAM is shown in the photograph (Fig.3).

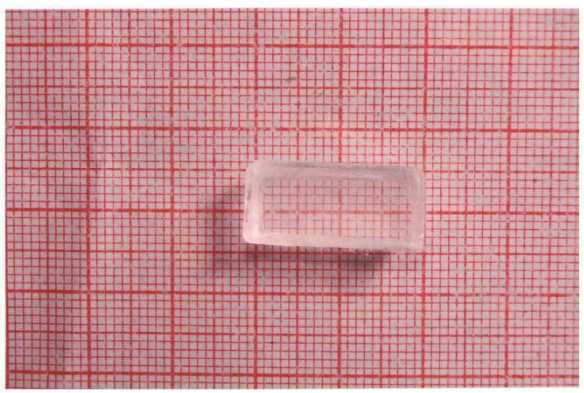

Fig. 3: A harvested crystal of L-alaninium maleate

5. Studies and Discussion

5.1 Structural studies

The grown crystal was subjected to single crystal X-ray diffraction studies using ENRAF NONIUS CAD4/MACH3 single crystal diffractometer with MoKα (λ=0.71069 Å) radiation to evaluate the lattice parameters. The obtained unit cell parameter are a=5.572(2) Å , b = 7.415(4) Å, c = 23.674(3) Å , $\alpha = \beta = \gamma = 90°$ and the volume of the unit cell is 978.12 Å. The XRD data proves that the LAM crystal crystallizes in orthorhombic structure with the space group $P2_1\ 2_1\ 2_1$ and the number of molecules in the unit cell is found to be 4.

5.2 Microhardness studies

The mechanical strength of LAM crystal was checked by carrying out microhardness studies by means of Leitz Vickers microhardness tester. The static indentations were made at room temperature with a constant indentation time of 10 s. The indentation marks were made by varying the load from 25 to 100 g. The variation of Vickers hardness number with the applied load for LAM sample is presented in the figure 4. It is observed from the figure that the hardness increases as the load increases. Cracks are formed beyond 100 g and the formation of cracks on the surface of the crystal beyond the load 100 g is due to the release of the internal stresses generated locally by indentation. The increase of microhardness with increasing load is in agreement with the Reverse Indentation Size Effect (RISE) as reported in the literature [14]

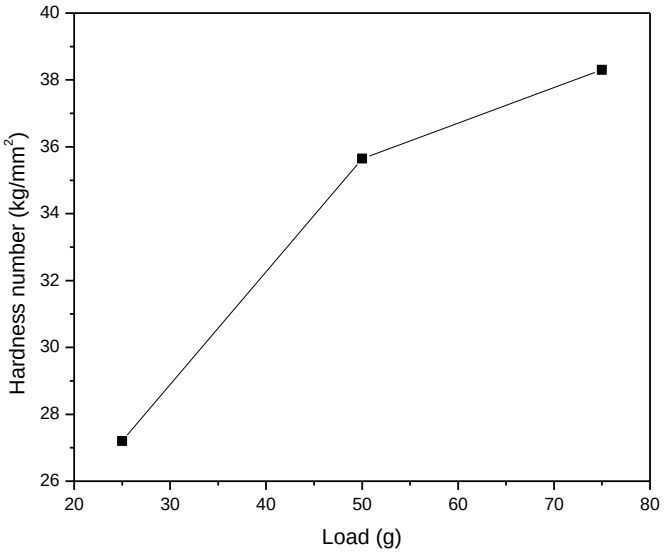

Fig.4: Dependence of hardness number with the applied load for LAM sample

The microhardness number (H_v) is related to yield strength (σ_y) by the equation $H_v = 3\sigma_y$ and the first order elastic stiffness constant (C_{11}) is related to the microhardness by the equation $\log C_{11} = (7/4) \log H_v$ [15,16] . The load dependence of yield strength and stiffness constant are provided in the table 2 and it is observed that the values of yield strength and stiffness constant increase with the applied load on the crystal.

Load (g)	Yield strength x 10^6 (pascal)	Stiffness constant x 10^{14} (pascal)
25 g	88.8	5.56
50 g	116.4	8.92
75 g	125.2	10.12

Table 2: Values of yield strength and stiffness constant for LAM sample

5.3 Measurement of density

Density can be calculated by knowing the mass of the unit cell content and the volume of the unit cell. Volume of the unit cell can be estimated from X-ray diffraction data. The measured density of a substance may sometimes be different from that estimated from the X-ray diffraction data. This is suggestive of crystal defects, mostly point defects in crystals leading to non-stiochiometry. Density of the crystal grown in the present study was measured by the floatation method [15] within an accuracy of ± 0.008 g/cm^3. Xylene (density: 0.864 g/cc) and carbon tetrachloride (density: 1.597 g/cc) were used for the experiment. After mixing the xylene and carbon tetrachloride in a suitable proportion in a specific gravity bottle, a small piece of crystal was immersed in a mixture of the liquids. When the sample was attained in a state of mechanical equilibrium, the density of the crystal would be equal to the density of mixture of liquids. The density was calculated using the relation

$\rho = (w3 - w1) / (w2-w1)$ where w1 is the weight of empty specific gravity bottle, w2 is the weight of the specific gravity bottle with full of water, and w3 is the weight of the specific gravity bottle full of the mixture of xylene and carbon tetrachloride. By the floatation method, the value of density of L-alaninium maleate crystal is found to be 1.392 g/cc.

5.4. Second Harmonic Generation (SHG) Test

Kurtz and Perry powder method is an important tool for searching for organic/semi organic/ inorganic NLO materials. In order confirm nonlinear optical property, microcrystalline form of LAM crystal was subjected to Kurtz and Perry powder test and Second Harmonic Generation (SHG) was confirmed by emission of green light (λ= 532 nm). The relative SHG efficiency for LAM sample was found to be 1.15 with respect to KDP and hence the sample of this work is a second harmonic generator of laser light.

5.5 Measurement of dielectric constant and dielectric loss

The dielectric constant determines the share of the electric stress which is absorbed by the material without any dielectric breakdown. Practically the presence of a dielectric between the plates of a condenser enhances the capacitance. This effect makes materials with high dielectric constant useful in capacitor technology. This enhancement of capacitance provides the basic experimental method for the measurement of dielectric constant. When an electric field acts on any matter the latter dissipates a certain quantity of electrical energy that transforms into heat energy. This phenomenon is commonly known as loss of power, meaning an average electric power dissipated in matter during a certain interval of time. The amount of power losses in a dielectric under the action of the voltage applied to it is commonly known as dielectric losses. The lower the dielectric loss the more effective is a dielectric material. Dielectric constant and dielectric loss values of crystalline samples were measured using a two-probe arrangement and an LCR meter. The measured values of dielectric constant and dielectric loss at different temperatures and at frequencies 10^3 Hz and 10^5 Hz presented in the figures 5 and 6. From the results of frequency and temperature dependence of dielectric parameters such as dielectric constant and loss factor, the dielectric parameters are observed to be decreasing with frequency and increasing with increase in temperature for L-alaninium maleate crystal. Higher values of dielectric constant at low frequencies may be due to the contributions mainly from space charge polarization. The space charge polarization depends on the purity and perfection of the material and its influence is noticeable in the low frequency region[16,17]. The orientational effect can some times be seen in some materials even up to 10^{10} Hz. Ionic and electronic polarizations exist below 10^{13} Hz. At higher frequencies, the values of dielectric constant and loss are low because molecules of larger relaxation times may not be able to respond to these higher frequencies. In accordance with Miller's rule, the lower value of dielectric constant at higher

frequencies is a suitable parameter for the enhancement of SHG coefficient [18]. The low value of dielectric loss at high frequency reveals the high optical quality of the crystal with lesser defects, which is the desirable property for NLO applications. It was observed that the dielectric constant increases with increase in temperature. The same behaviour is exhibited by dielectric loss (tan δ). Variation of the dielectric parameters of the sample with temperature is generally attributed to the crystal expansion, the electronic, space charge and ionic polarizations and also due to the thermally generated charge carriers[19,20].

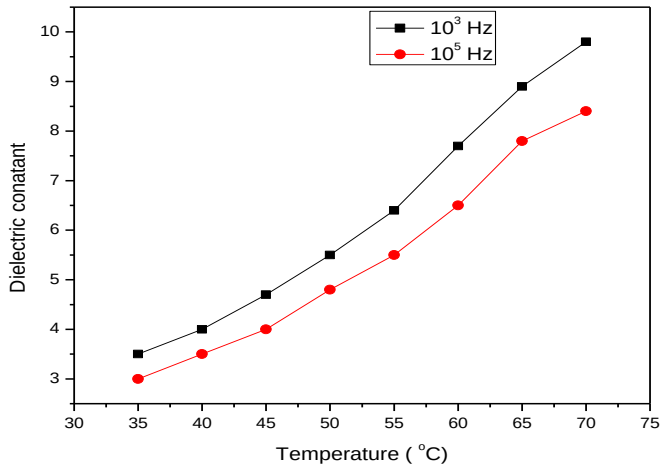

Fig.5: Temperature dependence of dielectric constant for LAM crystal

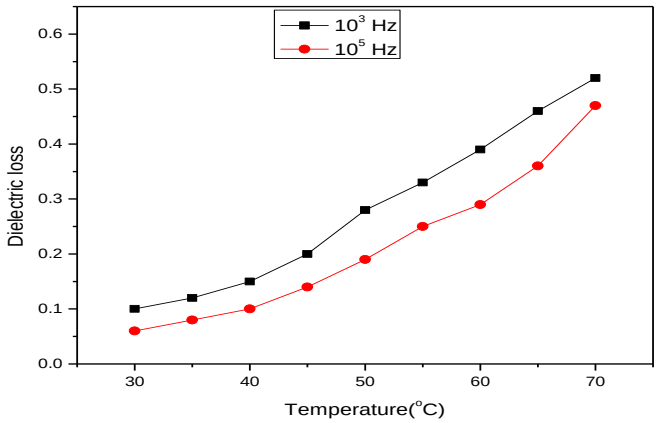

Fig.6: Temperature dependence of dielectric loss for LAM crystal

6.Conclusions

Solubility and nucleation kinetic studies were carried out for the synthesized L-alaninium maleate (LAM) salt and it is observed that the solubility in water increases with temperature and nucleation parameters were determined from the measured values of induction period. Using the value of supersturation ratio S= 1.1, the crystals of LAM have been grown by slow evaporation method. XRD reveals that the grown crystal crystallizes orthorhombic structure. The mechanical strength of the sample was analyzed by hardness studies and values of yield strength and stiffness constant were determined at different applied loads. SHG was tested by Kurtz powder method. The dielectric constant and loss factor values reveal that the grown LAM crystal is a suitable material for optical communication and opto-electronic technology.

Acknowledgement

The authors are thankful to the supported work from the various research institutions such as St Joseph College (Trichy), S. T. Hindu College (Nagercoil), Crescent Engineering College (Chennai) and M.K. University (Maduari). The authors are also grateful to authorities of managements of MDT Hindu College, Tirunelveli and Aditanar College of Arts and Science, Tiruchendur for the encouragement given to us to carry out the research work.

References

1. V. Bisder-Leib, M.F. Doherty, Cryst. Growth Des. 3 (2003) 221.
2. Thenneti Raghavalu, G. Ramesh Kumar, S. Gokul Raj, V. Mathivanan, R. Mohan, J. Crystal Growth 307 (2007) 112.
3. M. Diem, P.L. Polavarapu, M. Oboodi, L.A. Nafie, J. Am. Chem. Soc. 104 (1982) 3329.
4. A.S.J. Lucia Rose, P. Selvarajan, S. Perumal, Mater. Chem.Phys.130 (2011) 950.
5. Aravindan, P. Srinivasan, N. Vijayan, R. Gopalakrishnan, P. Ramasamy, Spectrochimica Acta Part A 71 (2008) 297.

6. Razzetti, M. Ardoido, L. Zanotti, M. Zha, C. Parorici, Cryst. Res. Technol. 37 (2002) 456.
7. V. Krishnakumar, R. Nagalakshmi, Spectrochimica Acta Part A 64(2006) 736.
8. M.Alagar, R.V. Krishnakumar, M.S. Nandhini, S. Natarajan, Acta Cryst. E57
9. (2001) o855.
10. D. Balasubramanian, R. Jayavel, P. Murugakoothan, Natural Science 1(2009) 216.
11. S. A. Natarajan, S. M. Britto, E. Ramachandran Crystal Growth & Design, 6 (2006)137.
12. P.Selvarajan, J.Glorium Arulraj, S.Perumal, J. Crystal Growth 311 (2009) 3835.
13. D. Shanthi, P. Selvarajan, K.K. HemaDurga, S. Lincy Mary Ponmani, Spectrochimica Acta Part A: 110 (2013) 1.
14. R.Jothi Mani, Dr.P.Selvarajan, Dr.H.Alex Devadoss and D.Shanthi, Int. J.Adv. Sci. Tech. Res. 3 (2013) 162.
15. J.H.Westbrook, H. Conard (Edn.), The Science of Hardness Testing and its Research Applications, American Society for Metals, Ohio (1973).
16. R. Wytt, "Metal Ceramics & Polymers", Cambridge University Press, London (1974).
17. W. A. Wooster, Widersande and Science Anwendung, Rep. Prog. Phys. 1(1953) 62.
18. P.Selvarajan, B.N.Das, H.B.Gon, K.V.Rao, J. Mater. Sci. 29 (1994) 4061.
19. R.C.Miller, Appl. Phys. Lett. 5 (1964) 17.
20. C.Krishnan, P.Selvarajan, S.Pari, Curr. Appl. Phys. 10 (2010) 664.
21. G.Ravi, G.Arunmozhi, S.Anbukumar, P.Ramasamy, Ferroelectrics 174 (1995) 241.